European Journal of Control 21 (2015) 27–35

Contents lists available at ScienceDirect

European Journal of Control

journal homepage: www.elsevier.com/locate/ejcon

Backstepping output-feedback control of moving boundary parabolic PDEs

Mojtaba Izadi, Stevan Dubljevic*

Department of Chemical and Materials Engineering, University of Alberta, Edmonton AB, Canada T6G 2V4

ARTICLE INFO

Article history:
Received 6 August 2014
Received in revised form
25 November 2014
Accepted 25 November 2014
Recommended by C. Prieur
Available online 4 December 2014

Keywords:
Parabolic PDE with time-varying domain
PDE backstepping observer design
Boundary control
Infinite-dimensional systems

ABSTRACT

This paper extends the backstepping-based observer design to the state estimation of parabolic PDEs with time-dependent spatial domain. The design is developed for the stabilization of a collocated boundary measurement and actuation of an unstable 1D heat equation with the application to the temperature distribution regulation in Czochralski crystal growth process. The PDE system that describes the estimation error dynamics is transformed to an exponentially stable target system through invertible transformations to obtain the time-varying kernel PDE defined on the time-varying triangular-shape domain. The exponential stability of the closed-loop system with an observer-based output-feedback controller is established by the use of a Lyapunov function. Finally, numerical solutions to the kernel PDEs and simulations are given to demonstrate successful stabilization of the unstable system.

1. Introduction

In the application of many control strategies, the knowledge of the state of the system is essential, yet, in most cases this information is not fully available due to reasons such as variables may not be measurable and using sensors may not be physically possible or economically justified. For these systems, a part of the design problem is the synthesis of state estimators (observers) that generate estimations of system states. Standard systematic techniques are available to design observers for linear and nonlinear finite-dimensional systems. However, for infinite-dimensional (or distributed-parameter) systems governed by partial differential equations (PDEs) the state variables do not depend only on time, but they also depend on spatial coordinates. In addition, changes in the shape and material properties characterized by phenomena such as material deformation, phase change, and mass transfer, may result in system models as moving boundary parabolic PDEs. Both infinite dimensionality and changes in the domain of these models impose further complexities and limitations to analysis and design.

One can address the observer (or controller) design problem for distributed parameter systems (DPSs) by using one of the two approaches: in the early-lumping method, at first the DPS is discretized by the use of suitable approximation techniques such as modal decomposition or Galerkin's method, to yield an approximate finite-dimensional model based on which state estimator is designed, see, e.g. [24,15]. However, this approximation may change the system properties such as observability and/or possibly induce the physical problem model failure. Moreover, stability of a closed-loop system cannot be established in general, and neglected dynamics may result in destabilization due to the observer spillover [3]. In the late-lumping approach, on the other hand, the designer takes full advantage of the physical nature of the process and uses available DPSs theory to design an observer for the PDE model, then the resulting observer is lumped for implementation. The works of [13,8,25,22,4,5,23] are notable in the generalization of the finite-dimensional systems observer theory to infinite-dimensional systems, more specifically the study of observability and detectability properties of DPSs. Along this line, several observer design methods are suggested in the literature including an extension of the Luenberger-type observer to PDE systems [7] and Lyapunov-based methods [20].

Another state estimation approach introduced by Smyshlyaev and Krstic [26] is the use of backstepping concept for boundary observation of PDE systems. In this methodology, an invertible Volterra integral transformation is used to transform the estimation error dynamics into a suitably selected stable distributed-parameter target system. The kernel of this transformation is defined by the solution of the so-called kernel PDE that is of a higher-order in space in the form of Klein–Gordon equation [19]. Having the solution of the kernel PDE, the observer gains can be found to be realized in the state estimator. From theoretical point of view, the technique of the PDE backstepping observer design is extended to the state estimation of unstable hyperbolic equations [18], compensation of sensor dynamics and/or PDE-ODE cascades [17,16,2], state estimation and output-feedback control for coupled PDE-ODE systems [27], linear parabolic PDEs with spatially- and time-varying

* Corresponding author at: Department of Chemical and Materials Engineering, University of Alberta, Edmonton AB, Canada T6G 2V4
E-mail address: stevan.dubljevic@ualberta.ca (S. Dubljevic).

http://dx.doi.org/10.1016/j.ejcon.2014.11.002
0947-3580/

reaction parameters [11], parabolic PDEs with nonlinear reactive-convective terms [12] and ultimately, observer design to semilinear parabolic PDEs [21].

In the case of a moving boundary parabolic PDE, even if the process parameters are time-invariant, the system is inherently nonautonomous [14]. Considering such problems as infinite-dimensional systems, direct state estimation is not possible in a large number of cases, because analytic expressions for the two-parameter semigroups describing the nonautonomous behavior of the system cannot be found. As an early-lumping approach, Galerkin's method is used for an eigenfunctions-based observer design in [1] for the boundary control of a 2D heat equation with time-dependent spatial domain.

Our recent work on the state-feedback boundary control of parabolic PDEs with time-varying domain using backstepping approach [9] motivates the observer design for the parabolic PDEs with time-varying domain. In this paper, the formulation to the PDE backstepping observer design for an unstable 1D heat equation described on a domain with moving boundaries is presented. The PDE system that governs the observation error dynamics is transformed to an exponentially stable target system through the Volterra-type integral transformation to obtain the kernel PDE, which has time-dependent parameters and is defined on the 2D time-varying domain. Then, the separation principle is validated, which provides exponential stability of the observer-based output-feedback controller setup. Finally, numerical solutions to the kernel PDEs and various simulations are given to demonstrate successful stabilization of an unstable system.

2. Problem statement

Consider the linear 1D parabolic PDE system of the form:

$$\partial_t \bar{x}(\xi,t) = \alpha \partial_\xi^2 \bar{x}(\xi,t) - \dot{h}(t)\partial_\xi \bar{x}(\xi,t) + \lambda_0 \bar{x}(\xi,t) \tag{1}$$

where $\bar{x}(\xi,t)$ is the state variable, $\mathbb{D}(t)=[0,h(t)]\subset\mathbb{R}$ is the time-varying domain of the definition of PDE, $\xi\in\mathbb{D}(t)$ is the spatial coordinate, $h(t)\in\mathbb{R}^+$ is the time-dependent length of the domain and $\dot{h}(t)$ is its time derivative, and $t\in[0,\infty)$ is the time. α and λ_0 are process parameters and the advection term appearing in (1) is due to the moving boundaries of the PDE domain [6,10]. The temperature distribution $\bar{x}(\xi,t)$ in the crystal of the Czochralski process or the shrinkage of a catalyst in a chemical process are two typical examples of the models that can be approximated by this PDE system. We assume the following boundary setting for the PDE system which is applicable to the temperature stabilization in the Czochralski crystal growth process:

$$\begin{aligned} &\bar{x}(0,t)=0\\ &\partial_\xi \bar{x}(h(t),t)=U(t) \end{aligned} \tag{2}$$

Here $U(t)$ is the control applied at the boundary $\xi=h(t)$ to stabilize the system state. For the design of the state observer, it is assumed that the output variable is given by

$$\bar{y}(t)=\bar{x}(h(t),t) \tag{3}$$

which characterizes the collocated measurement and actuation.

For the later analysis regarding the stability of the closed-loop system and boundedness and differentiability of the solutions the following assumption is required.

Assumption 1. The function $h(t)$ is analytic, i.e., there exists a real positive constant D such that for every non-negative integer j,

$$|\partial_t^j h(t)| \le D^{j+1} j! \tag{4}$$

To eliminate advection term in (1), the transformation $\bar{x}(\xi,t)=x(\xi,t)e^{\dot{h}(t)\xi/2\alpha}$ is used, which yields to the following PDE plant with associated boundary conditions:

$$\partial_t x(\xi,t) = \alpha\partial_\xi^2 x(\xi,t) + \lambda(\xi,t)x \tag{5}$$

$$\begin{cases} x(0,t)=0\\ \left[\partial_\xi x(h(t),t)+\dfrac{\dot{h}(t)}{2\alpha}x(h(t),t)\right]e^{h(t)\dot{h}(t)/2\alpha}=U(t) \end{cases} \tag{6}$$

where $\lambda(\xi,t)=\lambda_0-(\dot{h}^2(t)+2\ddot{h}(t)\xi)/4\alpha$. The output variable is transformed as well:

$$y(t)=x(h(t),t)=\bar{y}(t)e^{-h(t)\dot{h}(t)/2\alpha} \tag{7}$$

Also, for the stability analysis of moving-boundary PDEs, it is essential to define the L_2-norm of the function $w(\xi,t)$, $\xi\in\mathbb{D}(t)$ for the time-varying space $\mathbb{D}(t)$:

$$\|w(\xi,t)\| = \left(\int_0^{h(t)} w^2(\xi,t)\,d\xi\right)^{1/2} \tag{8}$$

Remark 1. The invertible space and time transformations:

$$\zeta=\frac{\xi}{h(t)},\quad \tau=\int_0^t \frac{ds}{h^2(s)}$$

maps the system (1 and 2) to

$$\partial_\tau \bar{x}(\zeta,\tau)=\alpha\partial_\zeta^2\bar{x}(\zeta,\tau)+\frac{dh(t(\tau))}{dt}h(t(\tau))(\zeta-1)\partial_\zeta\bar{x}(\zeta,\tau)+h^2(t(\tau))\lambda_0\bar{x}(\zeta,\tau)$$

$$\begin{cases} \bar{x}(0,\tau)=0\\ \dfrac{\partial_\zeta\bar{x}(1,\tau)}{h(t(\tau))}=U(t(\tau)) \end{cases}$$

The resulting PDE is a reaction–diffusion–advection system defined on the fixed domain $\zeta=[0,1]$ for which available formulations, as in [21], can be used. However, the length of the moving boundary domain $h(t)$ should be measured at each time instance in application. Since $h(t)$ appears in the space and time transformations, noisy measurement of this parameter affects highly the transformed PDE. This fact questions the robustness of synthesized controller or observer, and this method is not followed in this paper.

3. Backstepping state-feedback controller

The backstepping state-feedback results in [9] are frequently used in this work and they are briefly given in this section for easy reference.

The following state-feedback control law stabilizes the PDE system (5,6):

$$U(t)=\left(\int_0^{h(t)}\left[\frac{\dot{h}(t)}{2\alpha}k(h(t),\eta,t)+\partial_\xi k(\xi,\eta,t)\big|_{\xi=h(t)}\right]x(\eta,t)\;d\eta. \right.$$
$$\left. +k(h(t),h(t),t)x(h(t),t)\right)e^{h(t)\dot{h}(t)/2\alpha} \tag{9}$$

where the control gain function $k(\xi,\eta,t)$ is the kernel of the Volterra transformation:

$$w(\xi,t)=x(\xi,t)-\int_0^\xi k(\xi,\eta,t)x(\eta,t)\,d\eta \tag{10}$$

that transforms (5,6) to the following exponentially stable (in the sense of L_2-norm) PDE system:

$$\partial_t w(\xi,t)=\alpha\partial_\xi^2 w(\xi,t)-cw(\xi,t) \tag{11}$$

$$\begin{cases} w(0,t)=0 \\ \partial_\xi w(h(t),t)=-\dfrac{\dot h(t)}{2\alpha}w(h(t),t) \end{cases} \tag{12}$$

Based on the Assumption 1, the kernel function is the unique solution of the following kernel-PDE (see Appendix A):

$$\partial_t k(\xi,\eta,t)=\alpha(\partial_\xi^2 k(\xi,\eta,t)-\partial_\eta^2 k(\xi,\eta,t))-(\lambda(\eta,t)+c)k(\xi,\eta,t) \tag{13}$$

$$\begin{cases} k(\xi,0,t)=0 \\ k(\xi,\xi,t)=-\dfrac{1}{2\alpha}\int_0^\xi(\lambda(\eta,t)+c)\ d\eta \end{cases} \tag{14}$$

defined on the time-varying domain $\mathbb{S}_C(t)=\{(\xi,\eta)|0\le\eta\le\xi\le h(t)\}\subset\mathbb{R}^2$, see Fig. 1a. Exponential stability of the target system (11,12) implies exponential stability of the closed-loop plant (5,6,9) since (10) is invertible.

Remark 2. Although we developed the PDE backstepping formulation for specific boundary conditions, this approach can be adopted to other standard boundary conditions. For example, in the case of Dirichlet actuation $\bar x(h(t),t)=U(t)$, target system's boundary condition and control law would take the forms $w(h(t),t)=0$ and

$$U(t)=\left(\int_0^{h(t)}k(h(t),\eta,t)x(\eta,t)\ d\eta\right)e^{h(t)\dot h(t)/2\alpha},$$

respectively.

4. Observer design

In the following, a distributed-parameter Luenberger-type observer is designed by modifying the PDE system (5,6) with corrector terms as

$$\partial_t\hat x(\xi,t)=\alpha\partial_\xi^2\hat x(\xi,t)+\lambda(\xi,t)\hat x(\xi,t)+l(\xi,t)[y(t)-\hat x(h(t),t)] \tag{15}$$

$$\begin{cases} \hat x(0,t)=0 \\ \left[\partial_\xi\hat x(h(t),t)+\dfrac{\dot h(t)}{2\alpha}\hat x(h(t),t)\right]e^{h(t)\dot h(t)/2\alpha}=-l_0(t)[y(t)-\hat x(h(t),t)]+U(t) \end{cases} \tag{16}$$

where $l(x,t)$ and $l_0(t)$ are observer gain functions to be designed. The observer error $e(\xi,t)=x(\xi,t)-\hat x(\xi,t)$ satisfies the following PDE:

$$\partial_t e(\xi,t)=\alpha\partial_\xi^2 e(\xi,t)+\lambda(\xi,t)e(\xi,t)-l(\xi,t)e(h(t),t) \tag{17}$$

$$\begin{cases} e(0,t)=0 \\ \left[\partial_\xi e(h(t),t)+\dfrac{\dot h(t)}{2\alpha}e(h(t),t)\right]e^{h(t)\dot h(t)/2\alpha}=l_0(t)e(h(t),t) \end{cases} \tag{18}$$

In the subsequent sections, we are looking for the integral transformation:

$$e(\xi,t)=\tilde w(\xi,t)-\int_\xi^{h(t)}q(\xi,\eta,t)\tilde w(\eta,t)\ d\eta \tag{19}$$

that transforms (17,18) into the following exponentially stable (in the sense of the L_2-norm) target system:

$$\partial_t\tilde w(\xi,t)=\alpha\partial_\xi^2\tilde w(\xi,t)-\tilde c\tilde w(\xi,t) \tag{20}$$

$$\begin{cases} \tilde w(0,t)=0 \\ \partial_\xi\tilde w(h(t),t)=-\dfrac{\dot h(t)}{2\alpha}\tilde w(h(t),t) \end{cases} \tag{21}$$

with a free parameter $\tilde c\ge 0$ to manipulate the observer's convergence rate. Taking derivative of (19) with respect to space and time and substitution into (17,18) and performing intermediate computations yield to the time-varying PDE for the kernel function $q(\xi,\eta,t)$:

$$\partial_t q(\xi,\eta,t)=\alpha(\partial_\xi^2 q(\xi,\eta,t)-\partial_\eta^2 q(\xi,\eta,t))+(\lambda(\xi,t)+\tilde c)q(\xi,\eta,t) \tag{22}$$

$$\begin{cases} q(0,\eta,t)=0 \\ q(\xi,\xi,t)=-\dfrac{1}{2\alpha}\int_0^\xi(\lambda(\eta,t)+\tilde c)\ d\eta \end{cases} \tag{23}$$

and observer gains

$$\begin{aligned} l(\xi,t)&=\frac{\dot h(t)}{2}q(\xi,h(t),t)-\alpha\partial_\eta q(\xi,h(t),t) \\ l_0(t)&=q(h(t),h(t),t)e^{h(t)\dot h(t)/2\alpha} \end{aligned} \tag{24}$$

The kernel PDE (22,23) is defined on the time-varying domain $\mathbb{S}_O(t)=\{(\xi,\eta)|0\le\xi\le\eta\le h(t)\}\subset\mathbb{R}^2$, see Fig. 1b. Note that the form of PDE (22,23) is similar to (13,14) and the well-posedness and existence of the bounded solution to these kernel PDEs is shown in Appendix A.

The inverse backstepping transformation of (19) in terms of

$$\tilde w(\xi,t)=e(\xi,t)+\int_\xi^{h(t)}q_1(\xi,\eta,t)e(\eta,t)\ d\eta \tag{25}$$

with the kernel $q_1(\xi,\eta,t)$ maps (20,21) to (17,18) and it is straightforward to show that the PDE for the inverse kernel function is similar to (22,23) with a unique solution. Therefore, the invertibility of transformation (19) implies exponential stability of the error dynamics (17,18).

5. Output-feedback

The development of the exponentially convergent state estimator in previous section is independent of the control input. In this section, the observer is combined with the backstepping control to explore the output-feedback controller and establish separation principle, i.e., the incorporation of a separately designed state-feedback controller and

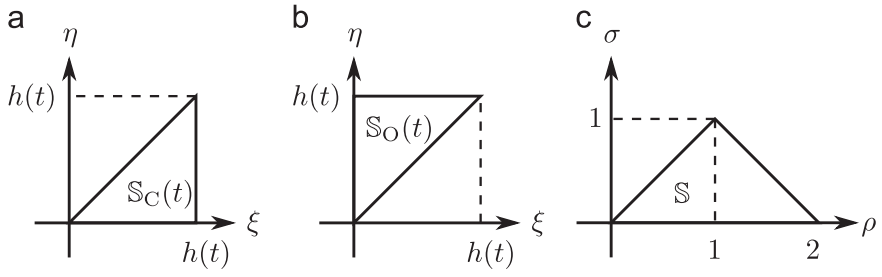

Fig. 1. (a) Time-dependent domain $\mathbb{S}_C(t)$ of the kernel function $k(\xi,\eta,t)$, (b) time-dependent domain $\mathbb{S}_O(t)$ of the kernel function $q(\xi,\eta,t)$ and (c) fixed domain $\mathbb{S}$ of functions $\bar k(\rho,\sigma,t)$ and $\bar q(\rho,\sigma,t)$.

observer results in a stabilizing output-feedback controller for the possibly unstable PDE with time-varying domain.

Consider the PDE plant (5,6) controlled by the following input based on the state observer (15,16):

$$U(t)=\left(\int_0^{h(t)}\left[\frac{\dot h(t)}{2\alpha}k(h(t),\eta,t)+\partial_\xi k(\xi,\eta,t)\big|_{\xi=h(t)}\right]\hat x(\eta,t)\,d\eta + k(h(t),h(t),t)\hat x(h(t),t)\right)e^{h(t)\dot h(t)/2\alpha} \tag{26}$$

Transformations

$$\hat w(\xi,t)=\hat x(\xi,t)-\int_0^\xi k(\xi,\eta,t)\,\hat x(\eta,t)\,d\eta \tag{27}$$

and (19) map the closed-loop system consisting of the observer PDE (15,16) and observation error PDE (17,18) into target systems

$$\partial_t\hat w(\xi,t)=\alpha\partial_\xi^2\hat w(\xi,t)-\hat c\hat w(\xi,t)+\left[l(\xi,t)-\int_0^\xi k(\xi,\eta,t)l(\eta,t)\,d\eta\right]\tilde w(h(t),t) \tag{28}$$

$$\begin{cases}\hat w(0,t)=0\\ \partial_\xi\hat w(h(t),t)+\dfrac{\dot h(t)}{2\alpha}\hat w(h(t),t)=-l_0(t)\tilde w(h(t),t)e^{-h(t)\dot h(t)/2\alpha}\end{cases} \tag{29}$$

and (20,21), respectively.

Theorem 1. *The system $(\hat w,\tilde w)$ is exponentially stable in the sense of L_2-norm for $\hat c\ge 1-\alpha/4D^2$ and $\tilde c\ge 1/2-(\alpha-D)/4D^2$.*

Proof. Consider the following Lyapunov function candidate:

$$V(t)=\frac{1}{2}\left(\|\hat w(\xi,t)\|^2+\beta\|\tilde w(\xi,t)\|^2\right) \tag{30}$$

where $\beta=\gamma_0^2+\gamma^2D$ with

$$\gamma_0=\alpha\left[\sup_t\left(l_0(t)e^{-h(t)\dot h(t)/2\alpha}\right)\right]$$
$$\gamma=\sup_{(\xi,t)}\left(l(\xi,t)-\int_0^\xi k(\xi,\eta,t)l(\eta,t)\,d\eta\right) \tag{31}$$

The fact that these functions are majorized by real constants γ and γ_0 is due to the boundedness of the solution to (22,23). Taking the time derivative of (30) and replacing from (28,20) yields

$$\begin{aligned}\dot V(t)=&\int_0^{h(t)}\hat w(\xi,t)\Big[\alpha\partial_\xi^2\hat w(\xi,t)-\hat c\hat w(\xi,t).\\ &+\left(l(\xi,t)-\int_0^\xi k(\xi,\eta,t)l(\eta,t)\,d\eta\right)\tilde w(h(t),t)\Big]d\xi+\frac{\dot h(t)}{2}\hat w^2(h(t),t)\\ &+\beta\int_0^{h(t)}\tilde w(\xi,t)\left[\alpha\partial_\xi^2\tilde w(\xi,t)-\tilde c\tilde w(\xi,t)\right]d\xi+\beta\frac{\dot h(t)}{2}\tilde w^2(h(t),t)\end{aligned}$$

Using integration by parts, applying boundary conditions (29,21) and imposing (31) results in

$$\begin{aligned}\dot V(t)\le&-\alpha\int_0^{h(t)}\left[\partial_\xi\hat w(\xi,t)\right]^2d\xi-\hat c\int_0^{h(t)}\hat w^2(\xi,t)\,d\xi\\ &-\gamma_0\hat w(h(t),t)\tilde w(h(t),t)\\ &+\gamma\int_0^{h(t)}\hat w(\xi,t)\tilde w(h(t),t)\,d\xi\\ &-\beta\alpha\int_0^{h(t)}\left[\partial_\xi\tilde w(\xi,t)\right]^2d\xi\\ &-\beta\tilde c\int_0^{h(t)}\tilde w^2(\xi,t)\,d\xi\end{aligned}$$

Note that Poincaré inequality takes the following form for any function $v(\xi,t)$ defined on the time-varying space $\mathbb{D}(t)$ (see Appendix B):

$$\int_0^{h(t)}v^2(\xi,t)\,d\xi\le 2h(t)v^2(0,t)+4h^2(t)\int_0^{h(t)}\left(\partial_\xi v(\xi,t)\right)^2d\xi \tag{32}$$

$$\int_0^{h(t)}v^2(\xi,t)\,d\xi\le 2h(t)v^2(h(t),t)+4h^2(t)\int_0^{h(t)}\left(\partial_\xi v(\xi,t)\right)^2d\xi \tag{33}$$

and one can show the following inequalities hold by the use of Young's, Poincaré and Cauchy–Schwartz inequalities for $\hat w(0,t)=0$ and $\tilde w(0,t)=0$:

$$\begin{aligned}-\gamma_0\hat w(h(t),t)\tilde w(h(t),t)\le&\frac{1}{4}\int_0^{h(t)}\hat w^2(\xi,t)\,d\xi\\ &+\gamma_0^2D\int_0^{h(t)}\left[\partial_\xi\tilde w(\xi,t)\right]^2d\xi\\ \gamma\int_0^{h(t)}\hat w(\xi,t)\tilde w(h(t),t)\,d\xi\le&\frac{1}{4}\int_0^{h(t)}\hat w^2(\xi,t)\,d\xi\\ &+\gamma^2D^2\int_0^{h(t)}\left[\partial_\xi\tilde w(\xi,t)\right]^2d\xi\end{aligned}$$

Therefore,

$$\begin{aligned}\dot V(t)\le&-\alpha\int_0^{h(t)}\left[\partial_\xi\hat w(\xi,t)\right]^2d\xi-\left(\hat c-\frac{1}{2}\right)\int_0^{h(t)}\hat w^2(\xi,t)\,d\xi\\ &-\left(\beta\alpha-\gamma_0^2D-\gamma^2D^2\right)\int_0^{h(t)}\left[\partial_\xi\tilde w(\xi,t)\right]^2d\xi\\ &-\beta\tilde c\int_0^{h(t)}\tilde w^2(\xi,t)\,d\xi\\ \le&-\left(\hat c-\frac{1}{2}+\frac{\alpha}{4D^2}\right)\int_0^{h(t)}\hat w^2(\xi,t)\,d\xi\\ &-\left(\beta\tilde c+\frac{\beta\alpha-\gamma_0^2D-\gamma^2D^2}{4D^2}\right)\int_0^{h(t)}\tilde w^2(\xi,t)\,d\xi\end{aligned}$$

Now choose $\hat c\ge 1-\alpha/4D^2$ and $\tilde c\ge 1/2-(\alpha-D)/4D^2$, hence

$$\dot V(t)\le-\frac{1}{2}\int_0^{h(t)}\hat w^2(\xi,t)\,d\xi-\frac{\beta}{2}\int_0^{h(t)}\tilde w^2(\xi,t)\,d\xi=-V(t)$$

Hence, the system $(\hat w,\tilde w)$ is exponentially stable. □

The system $(\hat x,e)$ is also exponentially stable since it is related to $(\hat w,\tilde w)$ by invertible backstepping transformations (19) and (27). This proves that the closed-loop system consisting of the plant with the backstepping controller and observer is exponentially stable.

6. Numerical solution to the kernel PDEs

To apply the control (26), one should know control and observer gains given in terms of kernels $k(\xi,\eta,t)$ and $q(\xi,\eta,t)$ that are described by associated PDEs (13,14) and (22,23), respectively. However, finding the solution to these equations on the time-dependent domains $\mathbb{S}_C(t)$ and $\mathbb{S}_O(t)$ is not straightforward. In this section, these PDEs are transformed to fixed spatial domains and then they are solved numerically.

Consider the space $\mathbb{S}=\{(\rho,\sigma)|0\le\sigma\le\rho\le 2-\sigma\}\subset\mathbb{R}^2$ given in Fig. 1c. The transformations $\mathcal{T}_C(t):(\xi,\eta)\in\mathbb{S}_C\mapsto(\rho,\sigma)\in\mathbb{S}$ given by

$$\rho=\frac{\xi+\eta}{h(t)},\quad \sigma=\frac{\xi-\eta}{h(t)} \tag{34}$$

and $\mathcal{T}_O(t):(\xi,\eta)\in\mathbb{S}_O\mapsto(\rho,\sigma)\in\mathbb{S}$ given by

$$\rho=\frac{\xi+\eta}{h(t)},\quad \sigma=\frac{-\xi+\eta}{h(t)} \tag{35}$$

map time-dependent domains $\mathbb{S}_C(t)$ and $\mathbb{S}_O(t)$ to the time-invariant space $\mathbb{S}$, respectively. Using $\mathcal{T}_C(t)$ and $\mathcal{T}_O(t)$, the kernel PDEs for $\overline{k}(\rho,\sigma,t)=k(\xi,\eta,t)$ and $\overline{q}(\rho,\sigma,t)=q(\xi,\eta,t)$ take the form:

$$\partial_t g(\rho,\sigma,t)=\delta\frac{4\alpha}{h^2(t)}\partial_\rho\partial_\sigma g(\rho,\sigma,t)+\frac{\dot{h}(t)}{h(t)}\left(\rho\partial_\rho g(\rho,\sigma,t)+\sigma\partial_\sigma g(\rho,\sigma,t)\right)$$
$$-\delta\left(\lambda\left(\frac{h(t)}{2}(\rho-\sigma),t\right)+\check{c}\right)g(\rho,\sigma,t) \tag{36}$$

$$\begin{cases} g(\rho,\rho,t)=0 \\ g(\rho,0,t)=f(\rho,t;\check{c}) \end{cases} \tag{37}$$

where $g(\rho,\sigma,t)=\overline{k}(\rho,\sigma,t)$, $\delta=1$ and $\check{c}=\hat{c}$ for (13,14) and $g(\rho,\sigma,t)=\overline{q}(\rho,\sigma,t)$, $\delta=-1$ and $\check{c}=\tilde{c}$ for (22,23). Also,

$$f(\rho,t;\check{c})=\frac{\rho h(t)}{4\alpha}\left[\frac{2\dot{h}^2(t)+\rho h(t)\ddot{h}(t)}{8\alpha}-(\lambda_0+\check{c})\right] \tag{38}$$

To numerically realize the solution to (36,37), the method of successive integration is utilized followed by numerical integration [11]. To this end, integrate (36) with respect to σ from 0 to σ and then with respect to ρ from σ to ρ and use boundary conditions (37) and integration by-parts for the terms with the first-order derivative to deduce (36,37) to the following integral equation:

$$\int_\sigma^\rho\int_0^\sigma\left[\partial_t g(\mu,\nu,t)+\left[2\frac{\dot{h}(t)}{h(t)}+\delta\left(\lambda\left(\frac{h(t)}{2}(\mu-\nu),t\right)+\check{c}\right)\right]g(\mu,\nu,t)\right]d\nu\,d\mu$$
$$-\frac{\dot{h}(t)}{h(t)}\left(\rho\int_0^\sigma g(\rho,\nu,t)\,d\nu+\sigma\int_\sigma^\rho g(\mu,\sigma,t)\,d\mu\right)$$
$$-\delta\frac{4\alpha}{h^2(t)}\left[g(\rho,\sigma,t)-f(\rho,t;\check{c})+f(\sigma,t;\check{c})\right]=0 \tag{39}$$

To find an approximate solution to (39), the integrals are approximated by the use of a composite trapezoidal rule. The triangular spatial domain $\mathbb{S}$ is discretized in N^2 computational points on an equally-spaced square grid as shown in Fig. 2. Hence, the continuous function $g(\rho,\sigma,t)$ is spatially discretized and denoted by $g_{i,j}(t)$ at the coordinate (ρ_i,σ_j) or simply at the point $(i,j)\in\{(m,n)|1\le n\le m\le 2N-n\}\subset\mathbb{N}^2$. Now, the integrals in (39) are approximated by using discrete values of their integrands evaluated at grid points through the application of the composite trapezoidal rule to obtain:

$$\frac{\Delta^2}{4}\sum_{i=J}^{I-1}\sum_{j=1}^{J-1}\left[\dot{g}_{i,j}+\dot{g}_{i+1,j}+\dot{g}_{i,j+1}+\dot{g}_{i+1,j+1}\right]$$
$$+\frac{\Delta^2}{4}\left(2\frac{\dot{h}(t)}{h(t)}+\delta\check{c}\right)\sum_{i=J}^{I-1}\sum_{j=1}^{J-1}\left[g_{i,j}+g_{i+1,j}+g_{i,j+1}+g_{i+1,j+1}\right]$$
$$+\delta\frac{\Delta^2}{4}\sum_{i=J}^{I-1}\sum_{j=1}^{J-1}\left[\overline{\lambda}_{i,j}g_{i,j}+\overline{\lambda}_{i+1,j}g_{i+1,j}+\overline{\lambda}_{i,j+1}g_{i,j+1}+\overline{\lambda}_{i+1,j+1}g_{i+1,j+1}\right]$$
$$-\frac{\Delta}{2}\frac{\dot{h}(t)}{h(t)}\left(\rho_I\sum_{j=1}^{J-1}\left[g_{I,j}+g_{I,j+1}\right]+\sigma_J\sum_{i=J}^{I-1}\left[g_{i,J}+g_{i+1,J}\right]\right)$$
$$-\delta\frac{4\alpha}{h^2(t)}\left[g_{I,J}-f(\rho_I,t;\check{c})+f(\sigma_J,t;\check{c})\right]=0 \tag{40}$$

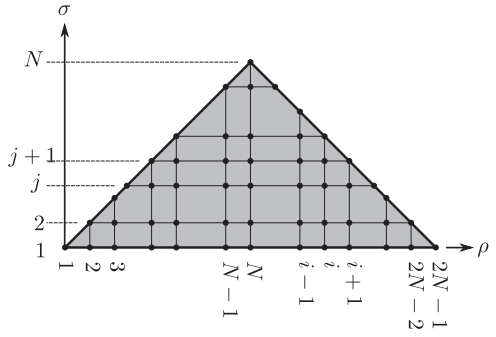

Fig. 2. Spatial discretization of the domain $\mathbb{S}$ of transformed kernel PDEs.

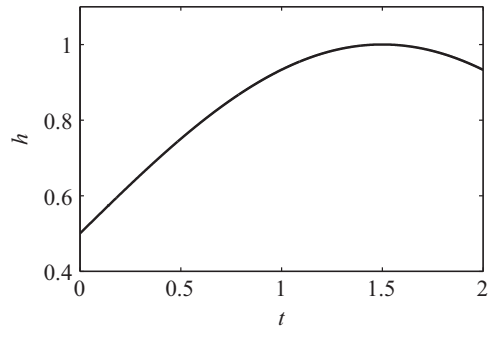

Fig. 3. Length $h(t)$ of the time-varying domain $\mathbb{D}(t)$ of the PDE system.

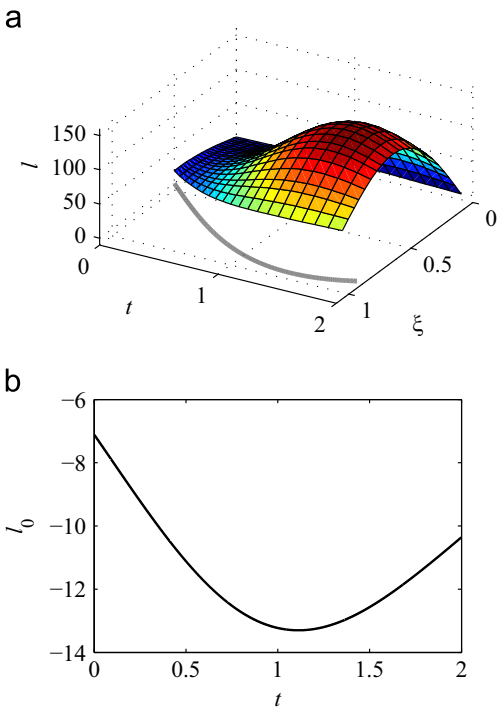

Fig. 5. (a) Observer gains $l(\xi,t)$ (the thick grey line shows the domain evolution) and (b) $l_0(t)$.

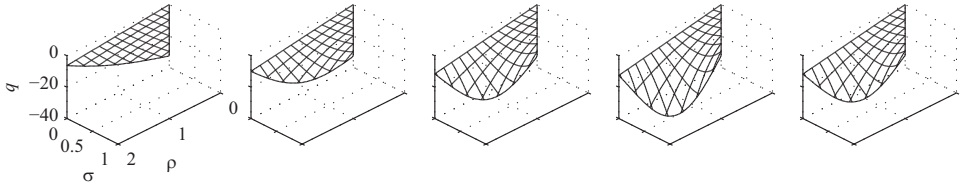

Fig. 4. The observer kernel function $q(\rho,\sigma,t)$ on the computational domain $\mathbb{S}$ at $t=0.0, 0.6, 0.95, 1.5$ and 2.0.

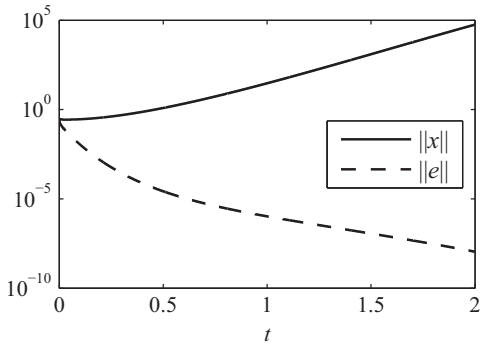

Fig. 6. Norms of the state and estimation error for the open-loop system.

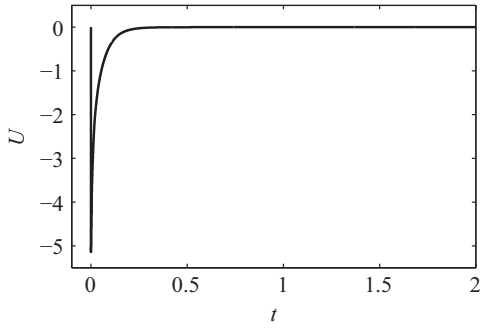

Fig. 7. Stabilizing control input.

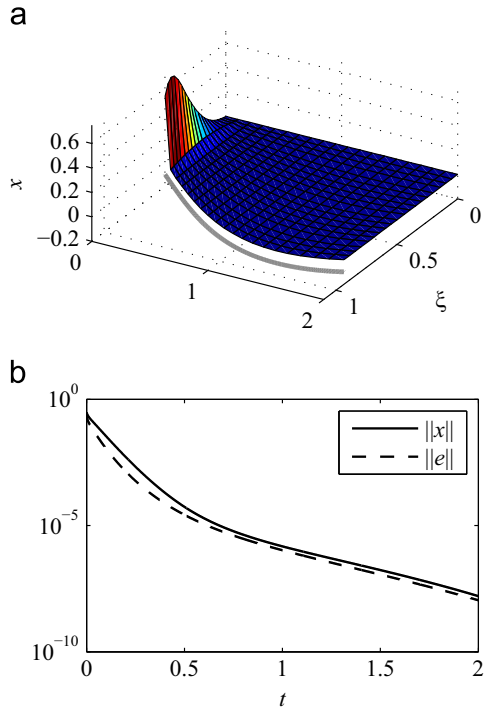

Fig. 8. (a) Closed-loop PDE system state evolution. (b) Norms of the state and estimation error for the closed-loop system.

where $\Delta = 1/(N-1)$ and $\overline{\lambda}_{i,j}(t) = \lambda(h(t)(\rho_i - \sigma_j)/2, t)$. For each pair (I,J) with unknown $g_{I,J}(t)$ (i.e., the points that are not on the boundaries with known boundary conditions), (40) relates the kernel function and its time derivative at computational points in the form of an ordinary differential equation (ODE). The new indexing $r = (2N-j)(j-1)+i$ will bijectively vectorize the array $g_{i,j}(t)$ into κ_r and the set of (N^2-3N+2) ODEs can be written in the following point-wise

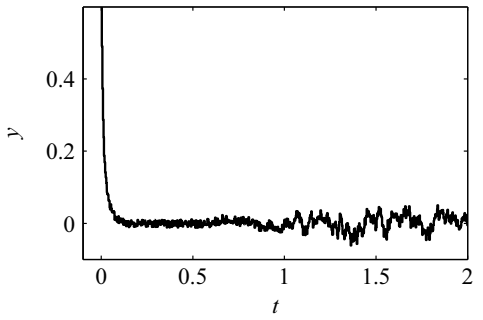

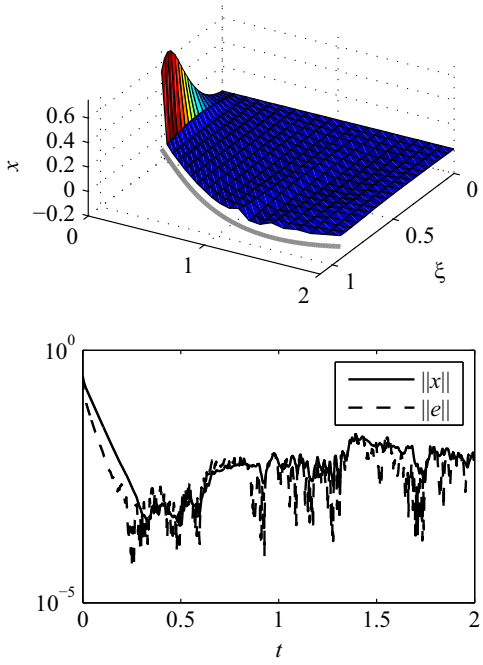

Fig. 9. Noisy measurements and the resulting closed-loop PDE system evolution.

equation:

$$A\dot{\kappa}(t) + B(t)\kappa(t) + H(t) = 0 \tag{41}$$

The initial condition $\kappa_0 = \kappa(0)$ for (41) is chosen as the stationary solution at $t=0$:

$$\kappa(0) = -B(0)^{-1}H(0) \tag{42}$$

Eqs. (41) and (42) can be considered as an initial-value problem in the form of a set of linear time-varying ODEs and can be solved efficiently using available numerical methods. Note that the definition of the new index r results in matrices A and $B(t)$ being in the lower triangular form.

7. Simulation results

The given approach to output-feedback control of the PDE system (5,6) is simulated and some results are shown in this section. Particularly, system parameters are $\alpha = 1$ and $\lambda_0 = 10$ and the change in the domain $h(t)$ is depicted in Fig. 3. The numerical discretization for the following simulations is obtained for $N=80$. The set of ODEs (41) is numerically realized using a first-order implicit integration scheme with $dt = 10^{-4}$.

Fig. 4 shows the numerical approximation of the time-varying observer kernel function $q(\rho, \sigma, t)$ on the computational domain $\mathbb{S}$ for $\hat{c} = \tilde{c} = 20$. The control gain kernel function $k(\rho, \sigma, t)$ has a very similar evolution profile. Observer gains $l(\xi, t)$ and $l_0(t)$ are

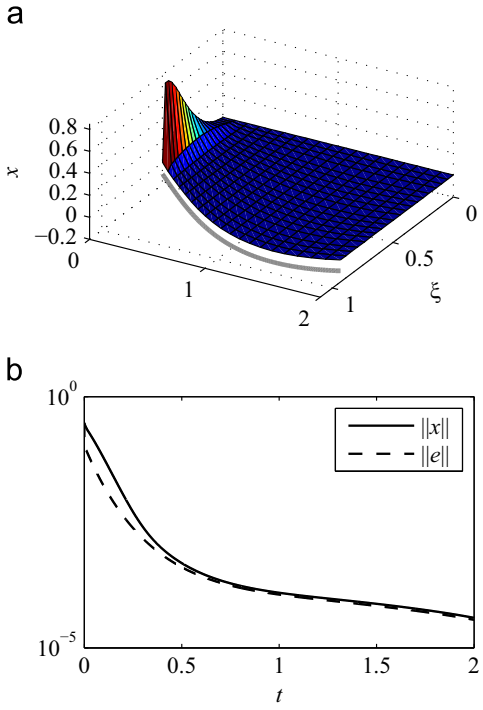

Fig. 10. (a) Closed-loop PDE system state evolution with reduced-order observer and (b) norms of the resulting state and estimation error.

computed numerically as given in (24) and are shown in Fig. 5. The solutions to the plant and observer PDEs are obtained by application of finite-difference method for the same discretization level N. Fig. 6 shows the norms of the PDE system state $x(\xi,t)$ and estimation error $e(\xi,t)$ for the open-loop system ($U(t)=0$) with arbitrary different initial conditions for the state $x(\xi,0)$ and observer $\hat{x}(\xi,0)$. It is seen that for given parameters the open-loop system is unstable, however, the observer converges exponentially to the plant.

The output-feedback control law (26) for the stabilization of the unstable PDE plant is shown in Fig. 7 where the observer initial state is zero. The spike in the control close to $t=0$ is due to a rather large estimation error at initial time instances. Fig. 8 shows the closed-loop evolution of the system state and L_2-norms of the state and estimation error. The exponential convergence of the observer as well as the stabilization of the unstable PDE system are well provided in the simulation results.

In previous results, it is assumed that continuous measurements are available during the process evolution. This assumption does not hold in many applications and sensors generate discrete measurements with noise. Fig. 9 shows system evolution when measurement is available every 20 time steps of the simulation and it is held during this period. In this case, control action is highly sensitive to noisy measurement because of the collocated measurement and actuation. However, the stabilization of the unstable plant is achieved by using the observer-based output-feedback controller.

As given by Eqs. (15,16), the Luenberger-type observer that estimates the system state is a distributed-parameter system. It is difficult/costly to physically realize such a system or numerically integrate because of its (high) infinite dimensionality. To circumvent this issue, a reduced-order finite-dimensional observer is considered by discretizing the observer PDE at the middle point ($\xi=h(t)/2$) and boundary points ($\xi=0$ and $\xi=h(t)$) at each time t. Given the boundary condition at $\xi=0$, the observer is now approximated by a second-order system when formulated by finite difference. Then the estimated state $\hat{x}(\xi,t)$ is constructed by a quadratic function passing through three computational points and evaluated at the original N grid points. The use of a two-dimensional observer in comparison to N-dimensional one reduces the computational time of the closed-loop system simulation by 32%.

Fig. 10 shows the plant stabilization based on the reduced-order observer design and evolution of the system state and L_2-norms of the state and estimation error. The observer error exponentially approaches zero, but at a slower rate in comparison to the higher-order observer given in Fig. 8 and the stabilization of the unstable PDE is accomplished.

8. Conclusions

The observer design of a 1D unstable heat equation on the time-varying domain is formulated in this work, where the observer gains are determined by the use of backstepping methodology. This includes a Volterra integral transformation to transform the estimation error PDE to a prescribed exponentially stable target system. The kernel function of this transformation is described by the 2D time-varying PDE on the moving boundary domain. Then, the designed observer is incorporated with the backstepping control in an output-feedback controller and the exponential stability of the closed-loop system is demonstrated by utilizing the Lyapunov theorem. Finally, numerical solutions to the kernel PDEs are provided and the output-feedback boundary stabilization of the unstable system is simulated to demonstrate the successful performance of the PDE with time-varying domain state estimator.

Acknowledgments

Financial support by Natural Science and Engineering Research Council of Canada (NSERC) Discovery Grant 386508-2011 is gratefully acknowledged.

Appendix A. Proof of the well-posedness of kernel PDEs

The well-posedness of kernel PDE (13,14) is shown here and (22,23) can be treated similarly. In Section 6 the PDE for kernel function $k(\xi,\eta,t)$ is transformed into the following equation:

$$\int_\sigma^\rho \int_0^\sigma \left[\partial_t k(\mu,\nu,t)+\left(2\frac{\dot{h}(t)}{h(t)}+\bar{\lambda}(\mu,\nu,t)\right)k(\mu,\nu,t)\right] d\nu\, d\mu - \frac{\dot{h}(t)}{h(t)}\left(\rho\int_0^\sigma k(\rho,\nu,t)\,d\nu+\sigma\int_\sigma^\rho k(\mu,\sigma,t)\,d\mu\right)-\frac{4\alpha}{h^2(t)}[k(\rho,\sigma,t) - f(\rho,t)+f(\sigma,t)]=0 \quad (A.1)$$

where

$$\bar{\lambda}(\rho,\sigma,t)=\lambda\left(\frac{h(t)}{2}(\rho-\sigma),t\right)+c$$

To show that this integral equation has a unique solution, the method of successive integration is used with Eq. (A.1) rewritten as

$$k(\rho,\sigma,t)=K_1(\rho,\sigma,t)+\mathcal{G}k(\rho,\sigma,t)$$

where

$$K_1(\rho,\sigma,t)=f(\rho,t)-f(\sigma,t)$$

$$\mathcal{G}k(\rho,\sigma,t)=\frac{h^2(t)}{4\alpha}\int_\sigma^\rho\int_0^\sigma \partial_t k(\mu,\nu,t)\,d\nu\,d\mu + \int_\sigma^\rho\int_0^\sigma\left(\frac{h(t)\dot{h}(t)}{2\alpha}+\frac{h^2(t)\bar{\lambda}(\mu,\nu,t)}{4\alpha}\right)k(\mu,\nu,t)\,d\nu\,d\mu - \frac{h(t)\dot{h}(t)}{4\alpha}\left(\rho\int_0^\sigma k(\rho,\nu,t)\,d\nu+\sigma\int_\sigma^\rho k(\mu,\sigma,t)\,d\mu\right) \quad (A.2)$$

The method of successive integration suggests that the solution to the integral equation (A.1) is given by the infinite series

$$k(\rho,\sigma,t)=\sum_{n=1}^{\infty}K_n(\rho,\sigma,t) \tag{A.3}$$

$$K_{n+1}(\rho,\sigma,t)=\mathcal{G}K_n(\rho,\sigma,t) \tag{A.4}$$

with $K_1(\rho,\sigma,t)$ given in (A.2).

Next we show by induction that the j-th time-derivative of K_n is bounded by

$$\sup_t\left|\partial_t^j K_n(\rho,\sigma,t)\right|\le\frac{3^{n+1}\gamma_{j,n}B^{j+2n}(j+n-1)!}{(n-1)!(n-1)!n!}(\rho\sigma)^{n-1} \tag{A.5}$$

where $B\ge 1$ is a real constant and

$$\gamma_{j,n}=\frac{\Gamma\left(\frac{4n+j}{3}+1\right)}{\Gamma\left(\frac{n+j}{3}+1\right)} \tag{A.6}$$

with $\Gamma(\zeta)$ being the gamma function. Following Assumption 1 one concludes that all functions $h(t)\dot{h}^2(t)/16\alpha^2$, $h^2(t)\ddot{h}(t)/32\alpha^2$, $h(t)(\lambda_0+c)/4\alpha$, $h^2(t)/4\alpha$, $h(t)\dot{h}(t)/2\alpha+h^2(t)\dot{\bar{\lambda}}(\rho,\sigma,t)/4\alpha$ are analytic as well. Hence, there exists real constant $B\ge 1$ such that the j-th time-derivative of these functions is bounded by $B^{j+1}j!$ for $j=0,1,2,\ldots$. Now, for $n=1$:

$$\begin{aligned}\sup_t\left|\partial_t^j K_1(\rho,\sigma,t)\right|&=\sup_t\left|\partial_t^j[f(\rho,t)-f(\sigma,t)]\right|\\&=\sup_t\left|\partial_t^j\left[\frac{h(t)\dot{h}^2(t)}{16\alpha^2}(\rho-\sigma)+\frac{h^2(t)\ddot{h}(t)}{32\alpha^2}(\rho^2-\sigma^2)-\frac{h(t)(\lambda_0+c)}{4\alpha}(\rho-\sigma)\right]\right|\\&\le B^{j+1}j!\left(|\rho-\sigma|+|\rho^2-\sigma^2|+|\rho-\sigma|\right)\le 8B^{j+1}j!\le 9\gamma_{j,1}B^{j+2}j!\end{aligned}$$

which is equal to the right-hand side of (A.5) for $n=1$. Assuming (A.5) holds for all $n=1,2,\ldots,N$, the upper bound of $\left|\partial_t^j K_{N+1}(\rho,\sigma,t)\right|$ can be determined as given in Box 1 which is identical to the right-hand side of (A.5) for $n=N+1$. This concludes the proof of (A.5).

Box 1–Series of inequalities to show (A.5) holds.

$$\begin{aligned}\sup_t|\partial_t^j K_{N+1}(\rho,\sigma,t)|&\le\sup_t\left|\partial_t^j\mathcal{G}K_N(\rho,\sigma,t)\right|\\&\le\sup_t\left|\sum_{i=0}^{j}\binom{j}{i}\partial_t^{j-i}\left(\frac{h^2(t)}{4\alpha}\right)\int_\sigma^\rho\int_0^\sigma\partial_t^{i+1}K_N(\mu,\nu,t)\,d\nu\,d\mu\right|+\\&\quad\sup_t\left|\sum_{i=0}^{j}\binom{j}{i}\int_\sigma^\rho\int_0^\sigma\partial_t^{j-i}\left(\frac{h(t)\dot{h}(t)}{2\alpha}+\frac{h^2(t)\dot{\bar{\lambda}}(\mu,\nu,t)}{4\alpha}\right)\partial_t^i K_N(\mu,\nu,t)\,d\nu\,d\mu\right|+\\&\quad\sup_t\left|\sum_{i=0}^{j}\binom{j}{i}\partial_t^{j-i}\left(\frac{h(t)\dot{h}(t)}{4\alpha}\right)\rho\int_0^\sigma\partial_t^i K_N(\rho,\nu,t)\,d\nu\right|+\\&\quad\sup_t\left|\sum_{i=0}^{j}\binom{j}{i}\partial_t^{j-i}\left(\frac{h(t)\dot{h}(t)}{4\alpha}\right)\sigma\int_\sigma^\rho\partial_t^i K_N(\mu,\sigma,t)\,d\mu\right|\\&\le\sum_{i=0}^{j}\binom{j}{i}B^{j-i+1}(j-i)!\frac{3^{N+1}\gamma_{i+1,N}B^{i+2N+1}(i+N)!}{(N-1)!(N-1)!N!}\left|\int_\sigma^\rho\int_0^\sigma(\mu\nu)^{N-1}d\nu\,d\mu\right|+\\&\quad\sum_{i=0}^{j}\binom{j}{i}B^{j-i+1}(j-i)!\frac{3^{N+1}\gamma_{i,N}B^{i+2N}(i+N-1)!}{(N-1)!(N-1)!N!}\left|\int_\sigma^\rho\int_0^\sigma(\mu\nu)^{N-1}d\nu\,d\mu\right|+\\&\quad\sum_{i=0}^{j}\binom{j}{i}B^{j-i+1}(j-i)!\frac{3^{N+1}\gamma_{i,N}B^{i+2N}(i+N-1)!}{(N-1)!(N-1)!N!}\left|\rho\int_0^\sigma(\rho\nu)^{N-1}d\nu\right|+\\&\quad\sum_{i=0}^{j}\binom{j}{i}B^{j-i+1}(j-i)!\frac{3^{N+1}\gamma_{i,N}B^{i+2N}(i+N-1)!}{(N-1)!(N-1)!N!}\left|\sigma\int_\sigma^\rho(\mu\sigma)^{N-1}d\mu\right|\\&\le\frac{3^{N+1}\gamma_{j+1,N}B^{j+2N+2}}{(N-1)!(N-1)!N!}\frac{(\rho\sigma)^N}{N^2}\sum_{i=0}^{j}\binom{j}{i}(j-i)!(i+N)!+\\&\quad\frac{3^{N+1}\gamma_{j,N}B^{j+2N+1}}{(N-1)!(N-1)!N!}\frac{(\rho\sigma)^N}{N^2}\sum_{i=0}^{j}\binom{j}{i}(j-i)!(i+N-1)!+\\&\quad\frac{3^{N+1}\gamma_{j,N}B^{j+2N+1}}{(N-1)!(N-1)!N!}\frac{(\rho\sigma)^N}{N}\sum_{i=0}^{j}\binom{j}{i}(j-i)!(i+N-1)!+\\&\quad\frac{3^{N+1}\gamma_{j,N}B^{j+2N+1}}{(N-1)!(N-1)!N!}\frac{(\rho\sigma)^N}{N}\sum_{i=0}^{j}\binom{j}{i}(j-i)!(i+N-1)!\\&\le\frac{3^{N+1}B^{j+2N+2}(j+N)!}{(N-1)!N!N!}(\rho\sigma)^N\left[\frac{\gamma_{j+1,N}(j+N+1)}{N(N+1)}+\frac{\gamma_{j,N}}{N^2}+2\frac{\gamma_{j,N}}{N}\right]\\&\le\frac{3^{N+1}B^{j+2N+2}(j+N)!}{N!N!N!}(\rho\sigma)^N\left[\frac{\gamma_{j+1,N}(j+N+1)}{N+1}+3\gamma_{j+1,N}\right]\\&=\frac{3^{N+1}B^{j+2N+2}(j+N)!}{N!N!(N+1)!}(\rho\sigma)^N\gamma_{j+1,N}(j+4N+4)=\frac{3^{N+2}\gamma_{j,N+1}B^{j+2N+2}(j+N)!}{N!N!(N+1)!}(\rho\sigma)^N\end{aligned}$$

In this sequence of inequalities used in Box 1, the following relations are used for $(\rho,\sigma)\in\mathbb{S}$, $j=0,1,2,\cdots$ and $n=1,2,\ldots$:

$|\rho-\sigma|\le 2$ and $|\rho^2-\sigma^2|\le 4$

$$\int_\sigma^\rho\int_0^\sigma(\mu\nu)^{n-1}d\nu\,d\mu=\frac{\sigma^n(\rho^n-\sigma^n)}{n^2}\le\frac{(\rho\sigma)^n}{n^2}$$

$$\rho\int_0^\sigma(\rho\nu)^{n-1}d\nu=\frac{(\rho\sigma)^n}{n}$$

$$\sigma\int_\sigma^\rho(\mu\sigma)^{n-1}d\mu=\frac{\sigma^n(\rho^n-\sigma^n)}{n}\le\frac{(\rho\sigma)^n}{n}$$

$$\gamma_{j,1}=\frac{j+1}{3}+1\ge 1$$

$\gamma_{i,n}\le\gamma_{j,n}$ for $i\le j$

$$\gamma_{j+1,n}(4n+j+4)=3\frac{\Gamma(\frac{4n+j+1}{3}+1)}{\Gamma(\frac{n+j+1}{3}+1)}\frac{(4n+j+4)}{3}=3\frac{\Gamma(\frac{4n+j+4}{3}+1)}{\Gamma\left(\frac{n+j+1}{3}+1\right)}=3\gamma_{j,n+1}$$

$$\sum_{i=0}^{j}\binom{j}{i}(j-i)!(i+n)!=\frac{(j+n+1)!}{n+1}$$

Now, let $j=0$ in (A.5) to find

$$\sup_t\left|K_n(\rho,\sigma,t)\right|\le 3\frac{\left(3B^2\right)^n\gamma_{0,n}}{(n-1)!n!}(\rho\sigma)^{n-1}$$

which provides the following bound for series (A.3):

$$|k(\rho,\sigma,t)|\le\sum_{n=1}^{\infty}|K_n(\rho,\sigma,t)|\le\sum_{n=1}^{\infty}3a_n(\rho,\sigma)$$

with

$$a_n(\rho,\sigma)=\frac{\left(3B^2\right)^n\gamma_{0,n}}{(n-1)!n!}(\rho\sigma)^{n-1}.$$

Hence, the ratio $|a_{n+1}(\rho,\sigma)/a_n(\rho,\sigma)|$ is

$$\frac{3B^2\rho\sigma}{n(n+1)}\frac{\gamma_{0,n+1}}{\gamma_{0,n}}$$

Having the limit

$$\lim_{n\to\infty}\frac{\gamma_{0,n+1}}{\gamma_{0,n}}=\lim_{n\to\infty}\frac{\Gamma\left(\frac{4n}{3}+\frac{7}{3}\right)\Gamma\left(\frac{n}{3}+1\right)}{\Gamma\left(\frac{4n}{3}+1\right)\Gamma\left(\frac{n}{3}+\frac{4}{3}\right)}=\lim_{n\to\infty}\frac{\Gamma\left(\frac{4n}{3}\right)\left(\frac{4n}{3}\right)^{7/3}\Gamma\left(\frac{n}{3}\right)\frac{n}{3}}{\Gamma\left(\frac{4n}{3}\right)\frac{4n}{3}\Gamma\left(\frac{n}{3}\right)\left(\frac{n}{3}\right)^{4/3}}$$
$$=\lim_{n\to\infty}(4n/3)^{4/3}\left(\frac{n}{3}\right)^{-1/3}=\lim_{n\to\infty}\frac{4\sqrt[3]{4}}{3}n$$

the series $\sum_{n=1}^{\infty}a_n(\rho,\sigma)$ is convergent since

$$\lim_{n\to\infty}\left|a_{n+1}(\rho,\sigma)/a_n(\rho,\sigma)\right|=\lim_{n\to\infty}\frac{4\sqrt[3]{4}B^2\rho\sigma}{n+1}=0<1$$

Therefore, the series (A.3) is absolutely convergent by comparison, which implies that integral equation (A.1) and eventually kernel PDE (13 and 14) have unique solutions.

Appendix B. Proof of Poincaré inequalities for the time-varying spaces

The proof to the conservative form of Poincaré inequality (32) for the time-varying space $\mathbb{D}(t)$ is given here, and (33) can be shown similarly. We start with the following relation:

$$v^2(\xi,t)=-\partial_\xi[(h(t)-\xi)v^2(\xi,t)]+2(h(t)-\xi)v(\xi,t)\partial_\xi v(\xi,t)$$

By integrating both sides of this equation with respect to ξ from 0 to $h(t)$ one obtains

$$\int_0^{h(t)}v^2(\xi,t)\,d\xi=h(t)v^2(0,t)+2\int_0^{h(t)}(h(t)-\xi)v(\xi,t)\partial_\xi v(\xi,t)\,d\xi$$
$$\le h(t)v^2(0,t)+\left(\int_0^{h(t)}v^2(\xi,t)\,d\xi\right)^{1/2}\left(\int_0^{h(t)}4(h(t)-\xi)^2\left(\partial_\xi v(\xi,t)\right)^2d\xi\right)^{1/2}$$
$$\le h(t)v^2(0,t)+\frac{1}{2}\int_0^{h(t)}v^2(\xi,t)\,d\xi+2\int_0^{h(t)}(h(t)-\xi)^2\left(\partial_\xi v(\xi,t)\right)^2d\xi \tag{B.1}$$

where Cauchy–Schwartz and Young's inequalities are used, respectively. One can readily show that these inequalities hold for the case of moving boundary space. The last integral in (B.1) is majorized by

$$\left[\sup_{\xi\in\mathbb{D}(t)}(h(t)-\xi)^2\right]\int_0^{h(t)}\left(\partial_\xi v(\xi,t)\right)^2d\xi=h^2(t)\int_0^{h(t)}\left(\partial_\xi v(\xi,t)\right)^2d\xi$$

resulting in the inequality (32).

References

[1] J. Abdollahi, M. Izadi, S. Dubljevic, Temperature distribution reconstruction in Czochralski crystal growth process, AIChE Journal 60 (8) (2014) 2839–2852.

[2] G. Antonio Susto, M. Krstic, Control of PDE-ODE cascades with Neumann interconnections, J. Frankl. Inst. 347 (1) (2010) 284–314.

[3] M.J. Balas, Active control of flexible systems, J. Optim. Theory Appl. 25 (3) (1978) 415–436.

[4] R.F. Curtain, H. Zwart, An Introduction to Infinite-dimensional Linear Systems Theory, Springer-Verlag, 1995.

[5] M.A. Demetriou, Natural second-order observers for second-order distributed parameter systems, Syst. Control Lett. 51 (3) (2004) 225–234.

[6] J. Derby, L. Atherton, P. Thomas, R. Brown, Finite-element methods for analysis of the dynamics and control of Czochralski crystal growth, J. Sci. Comput. 2 (4) (1987) 297–343.

[7] A. El Jai, M. Amouroux, Sensors and observers in distributed parameter systems, Int. J. Control 47 (1) (1988) 333–347.

[8] R.V. Gressang, G. Lamont, Observers for systems characterized by semigroups, IEEE Trans. Autom. Control 20 (4) (1975) 523–528.

[9] M. Izadi, J. Abdollahi, S. Dubljevic, PDE backstepping control of one-dimensional heat equation with time-varying domain, Automatica (2014), submitted for publication.

[10] M. Izadi, S. Dubljevic, Order-reduction of parabolic PDEs with time-varying domain using empirical eigenfunctions, AIChE J. 59 (11) (2013) 4142–4150.

[11] L. Jadachowski, T. Meurer, A. Kugi, An efficient implementation of backstepping observers for time-varying parabolic PDEs, in: The Proceedings of 7th International Conference on Mathematical Modelling, 2012, pp. 798–803.

[12] L. Jadachowski, T. Meurer, A. Kugi, State estimation for parabolic PDEs with reactive-convective non-linearities, in: The Proceedings of 12th European Control Conference (ECC), July 2013, pp. 1603–1608.

[13] S. Kitamura, S. Sakairi, M. Nishimura, Observer for distributed-parameter diffusion systems, Electr. Eng. Jpn. 92 (6) (1972) 142–149.

[14] P. Kloeden, P. Marín-Rubio, J. Real, Pullback attractors for a semilinear heat equation in a non-cylindrical domain, J. Differ. Equ. 244 (8) (2008) 2062–2090.

[15] T. Kobayashi, S. Hitotsuya, Observers and parameter determination for distributed parameter systems, Int. J. Control 33 (1) (1981) 31–50.

[16] M. Krstic, Compensating a string PDE in the actuation or sensing path of an unstable ODE, IEEE Trans. Autom. Control 54 (6) (2009) 1362–1368.

[17] M. Krstic, Compensating actuator and sensor dynamics governed by diffusion PDEs, Syst. Control Lett. 58 (5) (2009) 372–377.

[18] M. Krstic, B.-Z. Guo, A. Balogh, A. Smyshlyaev, Output-feedback stabilization of an unstable wave equation, Automatica 44 (1) (2008) 63–74.

[19] M. Krstic, A. Smyshlyaev, Boundary control of PDEs: a course on backstepping designs, SIAM, Philadelphia, 2008.

[20] Y. Liu, L. Lapdus, Observer theory for distributed-parameter systems, Int. J. Syst. Sci. 7 (7) (1976) 731–742.

[21] T. Meurer, On the extended Luenberger-type observer for semilinear distributed-parameter systems, IEEE Trans. Autom. Control 58 (7) (2013) 1732–1743.

[22] T. Nambu, On the stabilization of diffusion equations: boundary observation and feedback, J. Differ. Equ. 52 (2) (1984) 204–233.

[23] T.D. Nguyen, Second-order observers for second-order distributed parameter systems in R^2, Syst. Control Lett. 57 (10) (2008) 787–795.

[24] P.A. Orner, A.M. Foster, A design procedure for a class of distributed parameter control systems, J. Dyn. Syst. Meas. Control 93 (2) (1971) 86–92.

[25] Y. Sakawa, T. Matsushita, Feedback stabilization of a class of distributed systems and construction of a state estimator, IEEE Trans. Autom. Control 20 (6) (1975) 748–753.

[26] A. Smyshlyaev, M. Krstic, On control design for PDEs with space-dependent diffusivity or time-dependent reactivity, Automatica 41 (9) (2005) 1601–1608.

[27] S. Tang, C. Xie, State and output-feedback boundary control for a coupled PDE-ODE system, Syst. Control Lett. 60 (8) (2011) 540–545.